Bimodal behavior of the seasonal upwelling off the northeastern coast of Taiwan

Yu-Lin Chang,[1] Chau-Ron Wu,[1,2] and Lie-Yauw Oey[2]

Received 23 September 2008; revised 11 December 2008; accepted 26 January 2009; published 28 March 2009.

[1] Observations over the outer shelf and shelf break off the northeastern coast of Taiwan indicate a curious seasonal variability of upwelling. At deeper levels 100 m below the surface, upwelling is most intense in summer but weaker in winter. Nearer the surface at approximately 30 m below the surface, the opposite is true and the upwelling is stronger in winter than in summer. Results from a high-resolution numerical model together with observations and simple Ekman models are used to explain the phenomenon. It is shown that the upwelling at deeper levels (~100 m) is primarily induced by offshore (summer) and onshore (winter) migrations of the Kuroshio, while monsoonal change in the wind stress curl, positive in winter and negative in summer, is responsible for the reversal in the seasonal variation of the upwelling near the surface (~30 m). This mechanism reconciles previous upwelling data.

Citation: Chang, Y.-L., C.-R. Wu, and L.-Y. Oey (2009), Bimodal behavior of the seasonal upwelling off the northeastern coast of Taiwan, *J. Geophys. Res.*, *114*, C03027, doi:10.1029/2008JC005131.

1. Introduction

[2] The upwelling at the southern East China Sea (ECS) shelf is well known. The upwelling water is seen as a cold dome near the shelf break off the northeastern coast of Taiwan [*Fan*, 1980]. This is a region where exchanges between the Kuroshio water with the ECS shelf water take place. The Kuroshio enters the region along the eastern coast of Taiwan. After leaving Taiwan, the northward flowing Kuroshio bifurcates when colliding with the zonal running shelf break of the southern ECS defined by the 100~200 m isobath. The mainstream turns eastward following the topography, while a branch intrudes onto the shelf, bringing cold and nutrient-rich subsurface waters to the shelf of the southern ECS. The upwelling water contributes to the ECS a large amount of nutrients which are many times more than the deposits from the Yangtze River [*Chen*, 1996].

[3] Although the upwelling phenomenon has been extensively studied, the seasonal variation of the upwelling remained controversial. On the basis of chemical hydrography, *Liu et al.* [1992] found that the upwelling occurs year round and that it occasionally reaches the sea surface and becomes evident as a cold dome with nutrient-rich surface water. On the basis of a numerical study, *Chao* [1991] suggested that the path of the Kuroshio shifts with the seasons. During the northeast monsoon, the mainstream of the Kuroshio is closer to the shelf break while it shifts seaward during the southwest monsoon. The migration of the Kuroshio path may affect the upwelling which can therefore be seasonal. *Gong et al.* [1997] confirmed that the upwelling is a year-round phenomenon, and as the Kuroshio shifts shoreward in winter, the position of the upwelling center also shifts shoreward. *Tang et al.* [2000] used three shipboard acoustic Doppler current profilers to collect observations in different seasons from 1995 to 1997. They found upwelling during summer when the Kuroshio moves seaward but not during winter when the Kuroshio moves shoreward. On the basis of a numerical model simulation, *Wu et al.* [2008] indicated that upwelling exists year round below the depth of 150 m, but the eddy strengthens and weakens as the upper portion Kuroshio migrates seaward and shoreward, respectively.

[4] Recent nutrient data provide a somewhat different view about the seasonal variability. *Hsu* [2005] found that the upwelling intensified during winter and early spring on the basis of high nitrate and phosphate concentration in the euphotic zone. These observational nutrient data appear to contradict the earlier findings. The discrepancy deserves to be clarified and interpreted. However, the seasonal variability cannot be fully resolved from the existing data because of limited spatial and temporal coverage. In this study, the relationship between the upwelling and the nutrient data will be investigated using a fine grid resolution model with realistic topography and forcing. The behavior of the upwelling as well as their driving mechanisms will be discussed, and the apparent discrepancy between the nutrient data and previous work will be clarified. It will be shown that in addition to the Kuroshio migration, the wind stress curl plays an important role in modulating the seasonal variability of the upwelling.

2. Observations and Model Description

[5] Wind stress and wind stress curl are obtained from the Computational and Information System Laboratory research

[1]Department of Earth Sciences, National Taiwan Normal University, Taipei, Taiwan.
[2]Program in Atmospheric and Oceanic Sciences, Princeton University, Princeton, New Jersey, USA.

0148-0227/09/2008JC005131

data archive (available at http://dss.ucar.edu). The nutrient data NO_x are from cruise surveys [*Hsu*, 2005]. The data were collected from October 2003 to November 2004. Eight cruises were conducted on board R/V *Ocean Research II*, with six stations located off the northeastern coast of Taiwan, extending offshore from the upwelling region to the Kuroshio (Figure 1b). The NO_x concentration is measured over the euphotic zone. The depth of the euphotic zone is defined at the depth of 1% surface light penetration. Temperature and salinity used to calculate the stability in the upper ocean are obtained from conductivity-temperature-depth (CTD) deployed by National Center of Ocean Research (NCOR).

[6] The seas around Taiwan (SAT) model used here is the sigma coordinate Princeton Ocean Model [*Mellor*, 2004]. At the open boundaries, the SAT model derives its boundary conditions from a larger-scale East Asian Marginal Seas (EAMS) [*Wu and Hsin*, 2005] model (Figure 1a). The SAT model domain extends from 110.5°E to 126°E and from 13.5°N to 28°N (dashed box in Figure 1a). The horizontal grid size is 1/20°, and there are 26 sigma levels in the vertical. A detailed description of the SAT model has been given by *Wu et al.* [2008]. The SAT model was initialized by the temperature and salinity fields of the EAMS model outputs for January 1999 and was thereafter subjected to climatological forcing for 1 year. After this spin-up period, the SAT model was forced with NASA Quick Scatterometer/National Centers for Environmental Prediction (QSCAT/NCEP) wind data. The wind data are derived from spatial blending of high-resolution QSCAT–Direction Interval with Threshold Nudging (DIRTH) satellite scatterometer observations and the NCEP global reanalysis using a temporal resolution of 6 h and a spatial resolution of 0.5° × 0.5°. The simulation period was from 1999 to 2004.

3. Results

3.1. Mechanism Responsible for Seasonal Variability Shown in the Nutrient Data

[7] As mentioned in section 1, the nutrient data show a different seasonal variability than that found in earlier works. Figure 1b shows the model-derived flow and temperature pattern at a depth of 20 m on 1 May 1999. A cyclonic eddy of about 80 km in diameter is clearly visible off the northeastern coast of Taiwan. This cyclonic eddy, centered at about 25.35°N and 122.5°E, coincides with a region of lower temperature. The temperature near the eddy center was about 3°C lower than that of the ambient waters. At about 25°N, the northeastward flowing Kuroshio, with a maximum speed of over 100 cm/s, separates from the continental shelf break. A branch on the inshore side of the Kuroshio intrudes onto the continental shelf. This branch is impeded by the continental margin and turns westward to form a part of the cyclonic eddy. The cruise stations are shown in Figure 1b to extend offshore from the upwelling region. The NO_x concentrations were measured from cruises during the period from October 2003 to November 2004. The higher NO_x concentration is often observed at stations 9, 10, and 11, which coincides with the upwelling region.

[8] Figure 2 shows the NO_x concentration (red squares) together with the 30-day running mean modeled vertical velocity averaged in the top 30 m over the domain (blue box in Figure 1b) that encloses stations 9, 10, and 11. The NO_x data are also averaged in the upper 30 m over stations 9, 10, and 11 [*Hsu*, 2005]. Similar seasonal tendency is seen between the vertical velocity and NO_x concentration. The NO_x concentration is generally higher during winter and early spring when the model also shows intensified upwelling. The maximum nitrate concentration appears in early April 2004 near the maximum vertical velocity. By contrast, summer is low in NO_x coincident with the modeled weakened upwelling. The similarity between observed NO_x and modeled vertical velocity suggests that the model is capable of simulating the seasonal tendency of the near-surface upwelling (top 30 m) in the area.

[9] The 30-day running mean vertical velocities averaged over the blue box domain (Figure 1b) in the top 30 m during the period from 1999 to 2004 are shown in Figure 3. The values are positive in winter and negative in summer. This seasonal tendency is consistent with the NO_x data [*Hsu*, 2005] but appears to contradict the findings of *Tang et al.* [2000]. Prior to this study, the offshore migration of the Kuroshio in summer produced upwelling, and that is believed to be responsible for the seasonal variability of the upwelling in the region [*Tang et al.*, 2000]. The seasonal migration of the Kuroshio cannot, however, explain the seasonal tendency in the top 30 m over the study area (Figures 2 and 3). We propose a different mechanism. The surface layer is strongly affected by the wind, and it is plausible that the observed seasonal trend in the strength of upwelling is due to the seasonal variations of the wind stress curl reversal of the monsoonal winds. For example, *Gong et al.* [1992] found on the basis of hydrographic and satellite observations that the upwelling weakened under the lasting southwest monsoon in summer.

[10] We consider first the effects of wind. Since the time scales are long (seasonal), we assume steady (or quasi steady) state. The solution for total velocity (i.e., Ekman plus geostrophic) assuming a constant eddy viscosity is given by [e.g., *Gill*, 1982]

$$u_{\text{wind}} = \frac{e^{\zeta}}{\rho_o\sqrt{\nu f}}\left[\tau_o^x \sin\left(\zeta+\frac{\pi}{4}\right)+\tau_o^y \cos\left(\zeta+\frac{\pi}{4}\right)\right]+u_g \quad (1)$$

$$v_{\text{wind}} = \frac{e^{\zeta}}{\rho_o\sqrt{\nu f}}\left[-\tau_o^x \cos\left(\zeta+\frac{\pi}{4}\right)+\tau_o^y \sin\left(\zeta+\frac{\pi}{4}\right)\right]+v_g, \quad (2)$$

where $\zeta = \sqrt{f/2\nu}z$ and (u_g, v_g) is the geostrophic velocity outside the surface Ekman layer.

[11] The continuity equation then gives the vertical velocity

$$w_{\text{wind}}(\zeta) = \frac{1}{f\rho_o}\left[-e^{\zeta}\sin\zeta(\nabla\cdot\tau_o)+\left(1-e^{\zeta}\cos\zeta\right)(\nabla\cdot\tau_o)\right]. \quad (3)$$

Contours of the wind stress curl and divergence are shown in Figure 4 and Figure 5, respectively. The QSCAT/NCEP blended wind data set is one of the most up-to-date high-resolution data sets of ocean surface winds at the present time, and it is used to compute the wind stress curls and divergences. Summer is averaged over the period from May to July while winter is defined from October to December.

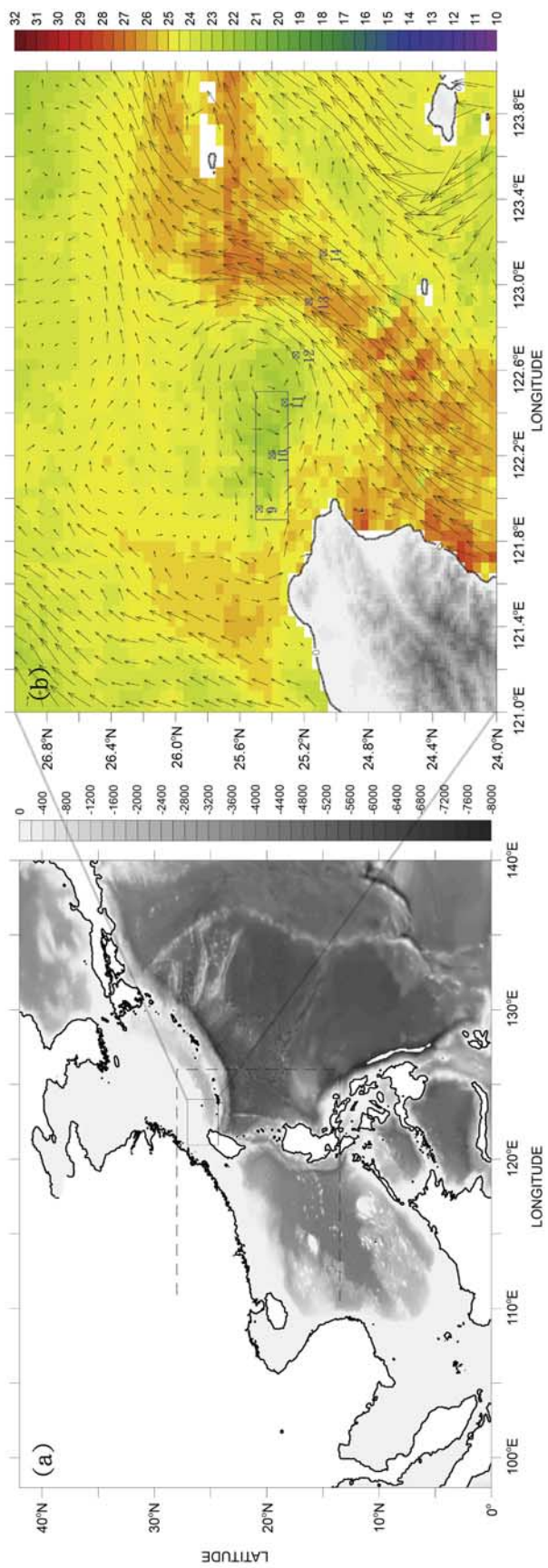

Figure 1. (a) The integrated domain of the EAMS and SAT (dashed box) model with realistic bathymetry. (b) Model-derived flow and temperature patterns at depth of 20 m on 1 May 1999. The blue box extends from 121.9°E to 122.5°E in longitude and from 25.3°N to 25.5°N in latitude. The squares are the location of stations. The red dashed contour indicates the 200 m isobath.

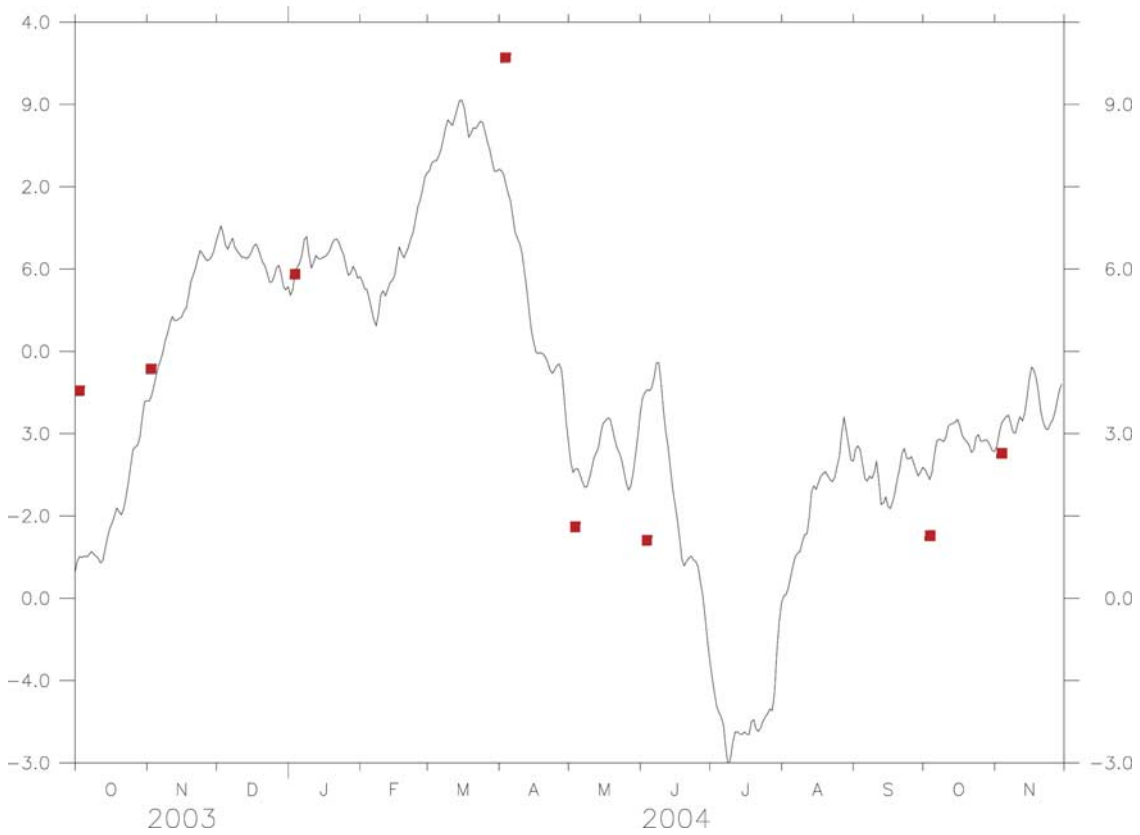

Figure 2. NO_x concentration (red squares) [from *Hsu*, 2005] together with the averaged modeled vertical velocity of 30-day running mean in the top 30 m over the blue box domain of Figure 1b.

The wind stress curl is negative in summer but positive in winter off the northeastern coast of Taiwan (Figure 4), suggesting that upwelling induced by the wind stress curl occurs only in winter. On the other hand, the wind stress divergence is weakly positive in summer but is negative in winter over the upwelling area (Figure 5). The strong convergence near the northeastern coast of Taiwan during winter may be due to the effects of local orography on the northeast monsoon. Equation (3) is used to estimate w_{wind} for both summer and winter (Figure 6). The eddy viscosities used here are averaged from the surface to the depth of 100 m and are taken from the numerical model; they are 0.015 m^2/s and 0.0042 m^2/s for winter and summer, respectively. For these eddy viscosity values, the 1/e decay depth (which is proportional to the Ekman depth, which equals $\sqrt{2\nu/f}$) is approximately 10∼23 m, so the effects of wind divergence term on the vertical velocity are small below this depth. The w_{wind} is negative in the upper 100 m in summer. In winter, w_{wind} is negative very near the surface forced by the strong wind stress convergence but becomes positive at approximately 23 m below the surface. The results illustrate clearly the seasonal tendency in the top layer related to the wind, which generates upwelling for depths deeper than 20∼30 m in winter and downwelling throughout the surface layer in summer.

[12] In addition to the wind forcing, strong stratification also affects vertical motions. Different stratifications have been observed in the study region during winter and summer. The temperature data from NCOR shows deeper mixed layer in winter than in summer (Figure 7a). The CTD casts were located between stations 10 and 11 (Figure 1b) in the upwelling domain at (122.25°E, 25.33°N) on 9 June 1999 and at (122.25°E, 25.42°N) on 10 November 1999. In winter, the upper layer is well mixing and the mixed layer depth is about 65 m because of strong northeasterly monsoon and surface cooling. By contrast, the mixed layer is only 20 m in summer because of the weak southwesterly monsoon and strong surface heating. Buoyancy frequency squared calculated from the observed temperature and salinity data also shows a similar seasonality (Figure 7b). The maximum buoyancy frequency squared is found at a depth of 20 m in summer but deeper at 70 m in winter. The eddy viscosity in summer is also smaller. Thus, summer stratification prohibits vertical mixing near the surface and reduces the Ekman depth ($\sqrt{2\nu/f}$); wind-induced downwelling velocity then reaches its full strength at a shallow depth $z \approx -30$ m (Figure 6).

3.2. Bimodal Behavior of the Seasonal Upwelling

[13] Figure 6 shows that below a near-surface layer of about 20 m, the wind tends to induce upwelling in winter but downwelling in summer. This is contrary to the findings of *Liu et al.* [1992], who pointed out that the upwelling is a year-round phenomenon. Clearly, wind-driven upwelling and downwelling alone cannot explain the observations. *Gong et al.* [1997] found that as the Kuroshio moves shoreward in winter, the center of upwelling also moves shoreward. In summer, the center of upwelling shifts

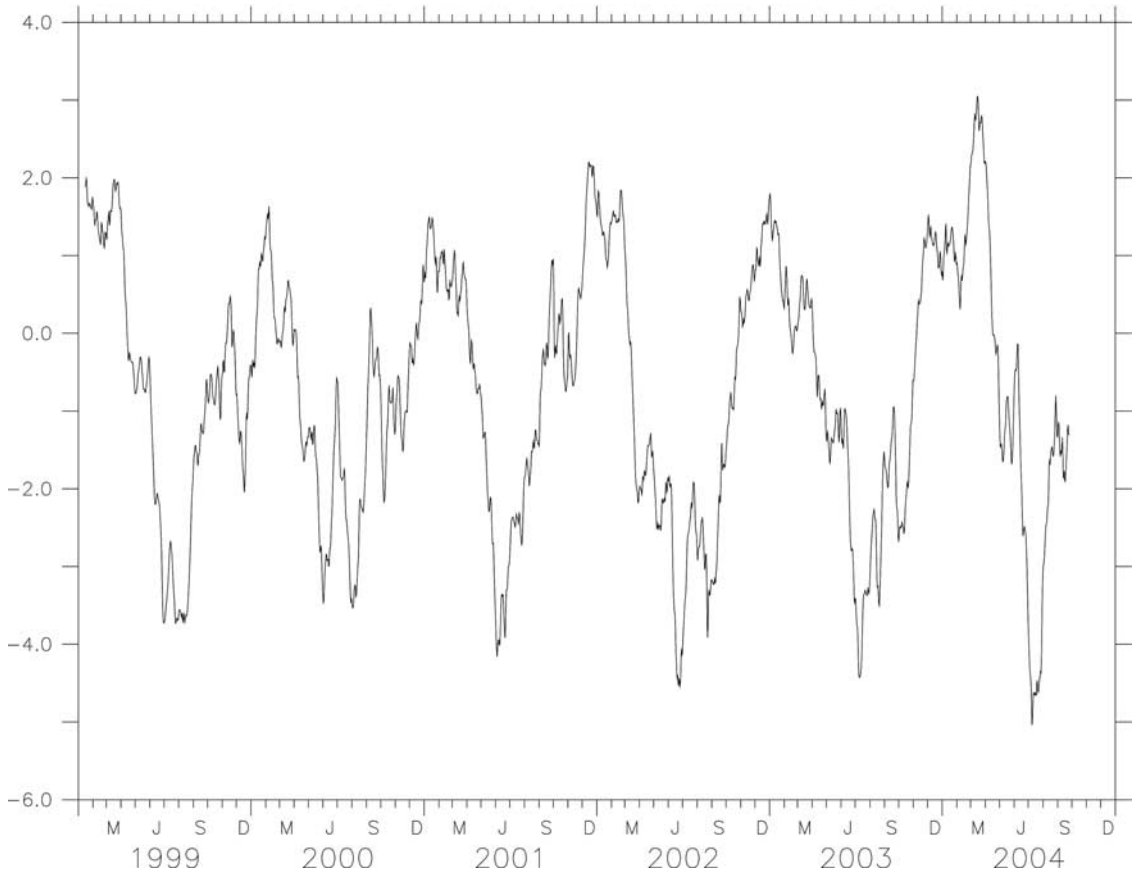

Figure 3. The daily vertical velocity of 30-day running mean during the period from 1999 to 2004 in blue box of Figure 1b.

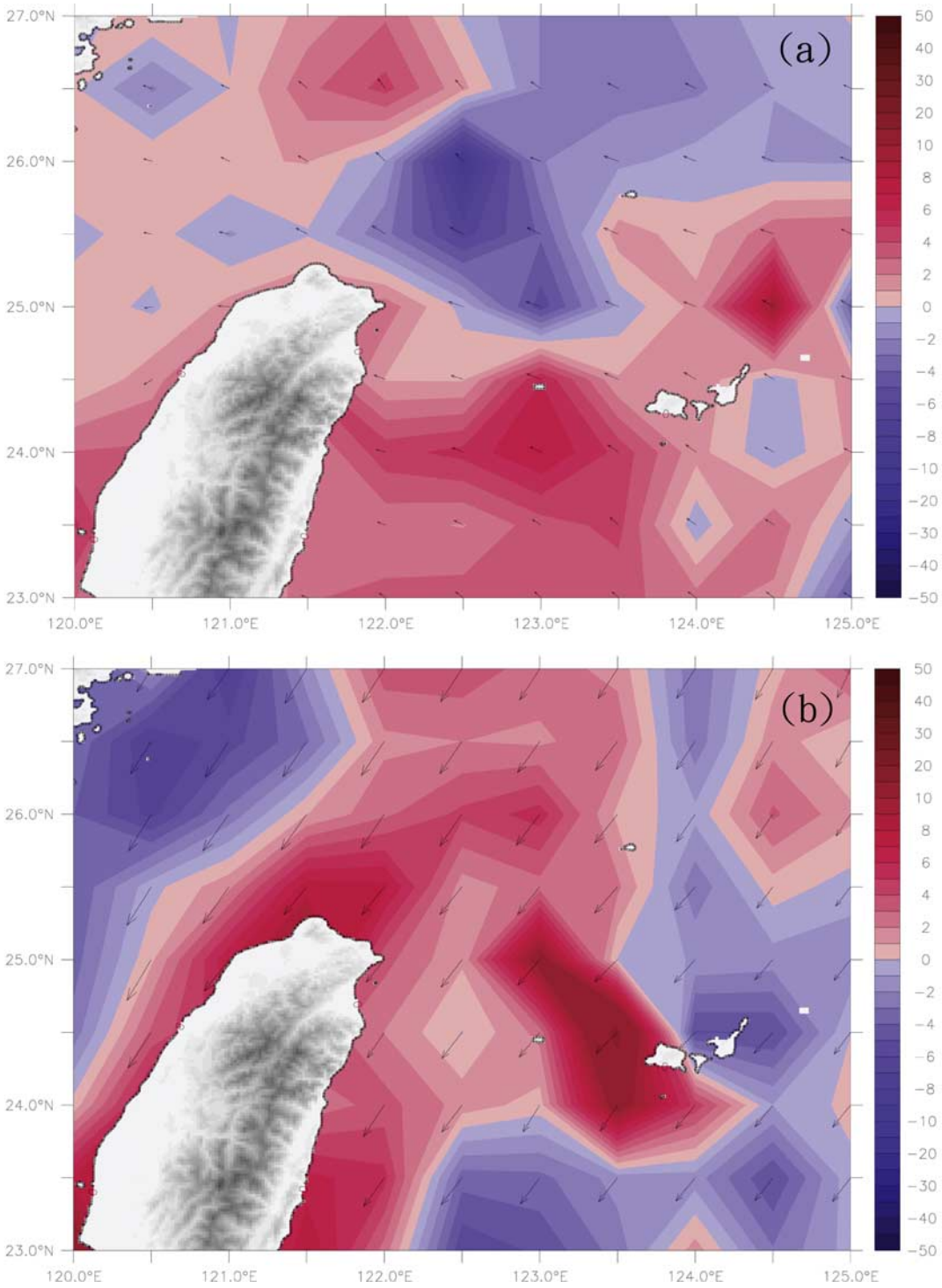

Figure 4. Averaged wind stress curl with wind field during the period from 1999 to 2004 in (a) summer and (b) winter.

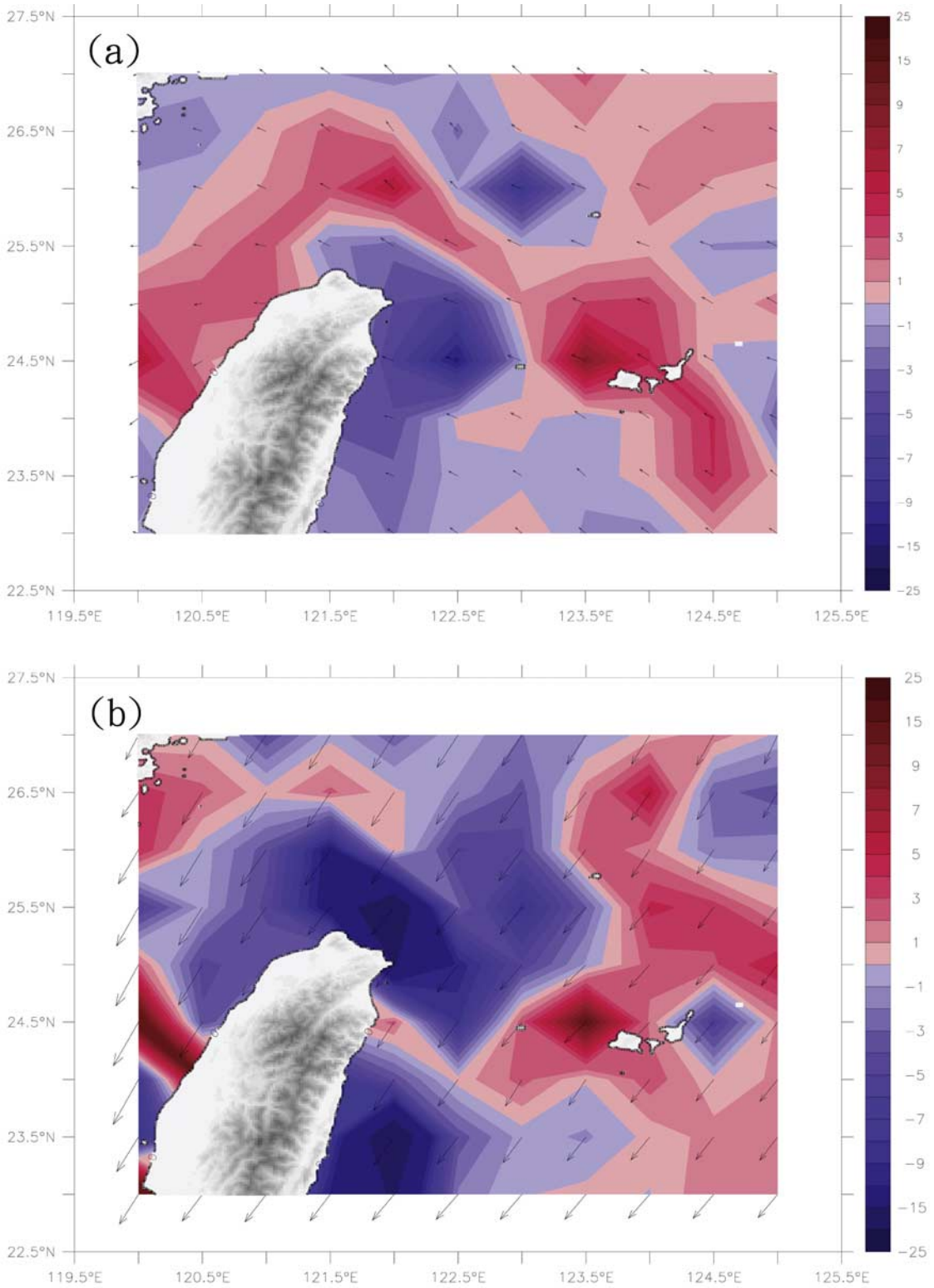

Figure 5. Averaged divergence with wind field during the period from 1999 to 2004 in (a) summer and (b) winter.

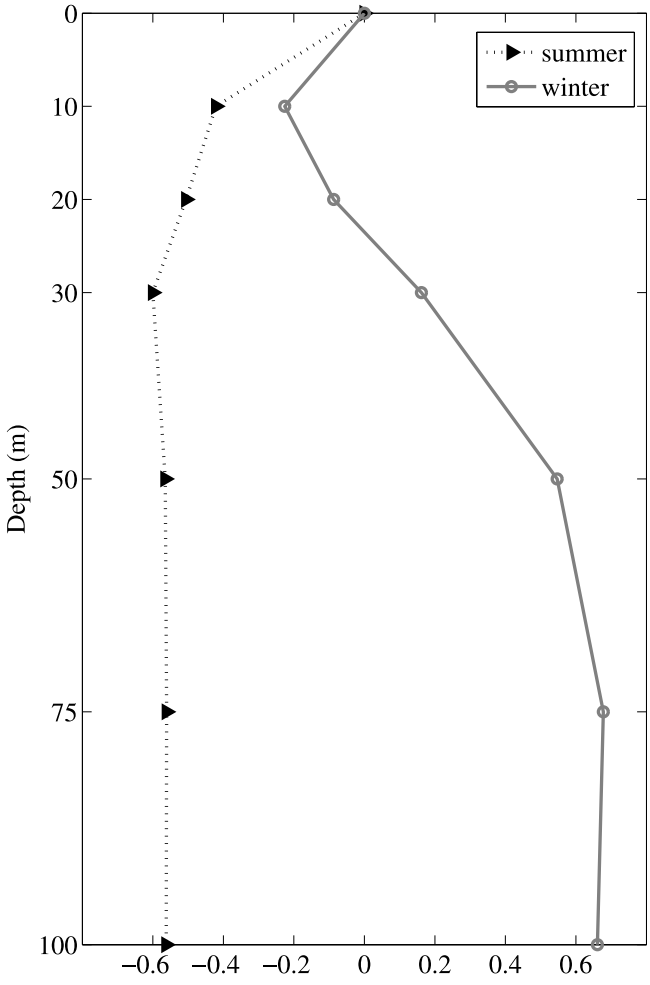

Figure 6. The vertical velocity w_{wind} in the upper 100 m in summer (dashed line) and in winter (solid line) in blue box of Figure 1b.

seaward as the Kuroshio moves seaward. Thus, the upwelling shifts between the continental shelf and the slope in response to the migration of the Kuroshio. This seasonal shift of the Kuroshio is seen also in the model results. Figure 8 shows contours of along-Kuroshio velocity at a section that spans the region of upwelling averaged from 1999 to 2004 (Figure 8a). In summer (Figure 8b), the western edge of the Kuroshio near the surface is farther offshore than in winter (Figure 8c). This seasonal variability may be due to the reversal of monsoon wind [*Chao*, 1991; *Wu et al.*, 2008], but it may also be due to the seasonal variation of stratification interacting with topography (the so-called "joint effect of baroclinicity and relief effects") [*Kagimoto and Yamagata*, 1997]. Whatever the cause, the modeled upwelling also responds to this seasonal shift in Kuroshio (Figure 8).

[14] Figure 9 shows seasonal variation of modeled vertical velocity in the upper 100 m in the upwelling domain defined as 122.25°∼122.75°E and 25.1°∼25.6°N. This domain, which is different from the blue box in Figure 1b, is based on a visual inspection of the model cyclonic flow pattern at the inshore edge of Kuroshio, showing the case as upwelling shift to the slope and affected by the Kuroshio more apparently. On the basis of chemical hydrography, *Liu et al.* [1992] estimated an upwelling rate of 5.4 m/d in the upper 60 m on the basis of a box model calculation. From the model, the average upwelling rate over the 6-year period is 5.44 m/d in the upper 60 m. These values agree with the estimates of *Liu et al.* [1992]. Moreover, Figure 9 shows that the values of the averaged vertical velocity in the upwelling area are positive throughout the year in the upper 100 m, indicating that the upwelling is a year-round phenomenon which confirms the findings by *Liu et al.* [1992].

[15] Figure 9a reveals a bimodal behavior of the vertical velocity in the water column, a characteristic which we propose below is caused by the interplay between the Kuroshio and wind-induced upwelling in different portions of the water column in different seasons. The upwelling in the top layer (∼30 m) is stronger in winter but weaker in summer. The lower layer displays an opposite tendency, showing a stronger upwelling in summer than in winter. This bimodal behavior is apparent when the vertical velocity is averaged from the surface to a depth of z. Figure 9b shows the monthly vertical velocity averaged in the upper 100 m (open square), in the top 30 m (cross), and in the upper 60 m (open triangle). Graphically, the values averaged in the upper 60 m show no clear seasonal variation and range from 4.9∼6.0 m/d; the modeled averaged vertical velocity in March is 5.9 m/d, which is in agreement with *Liu et al.*'s [1992] estimate for the same month. The vertical velocities averaged in the upper 100 m and in the top 30 m (Figure 9b) show different seasonal variability. The averaged upwelling in the upper 100 m in summer is stronger than in winter. The model seasonal variability at deeper levels agrees with observed variability [e.g., *Gong et al.*, 1997; *Tang et al.*, 2000]. On the contrary, the upwelling averaged in the top 30 m is stronger in winter than in summer. Different mechanisms are therefore responsible for the seasonal upwelling near the surface and at deeper levels. The model results suggest that seasonal upwelling at the deeper level is controlled by the onshore (winter) and offshore (summer) movements of the Kuroshio [*Wu et al.*, 2008] (Figure 8). On the other hand, the migration of the Kuroshio cannot explain the seasonal upwelling in the top 30 m. Near the surface, effects of wind stress curl and divergence cannot be ignored. As shown previously, their effects are limited to the top 30 m of the water column (Figure 6) and result in stronger upwelling in winter than in summer (Figure 9b).

[16] These ideas may be explained by splitting the vertical velocity into the sum of the velocity due to the Kuroshio and the velocity due to the wind:

$$w_{\text{total}} = w_{\text{kuroshio}} + w_{\text{wind}}. \tag{4}$$

Here, we lump into w_{kuroshio} effects of the Kuroshio and of any interaction between the Kuroshio and wind (through the mechanism discussed, for example, by *Chao* [1991]). The w_{total} is from the circulation model, and we estimate w_{wind} using equation (3). Figure 10 shows the averaged monthly anomalies of w_{kuroshio} (dashed line, mean = 7.5 m/d) and w_{wind} (solid line, mean = −0.3 m/d) averaged from the surface to a depth of 100 m for the period from 1999 to

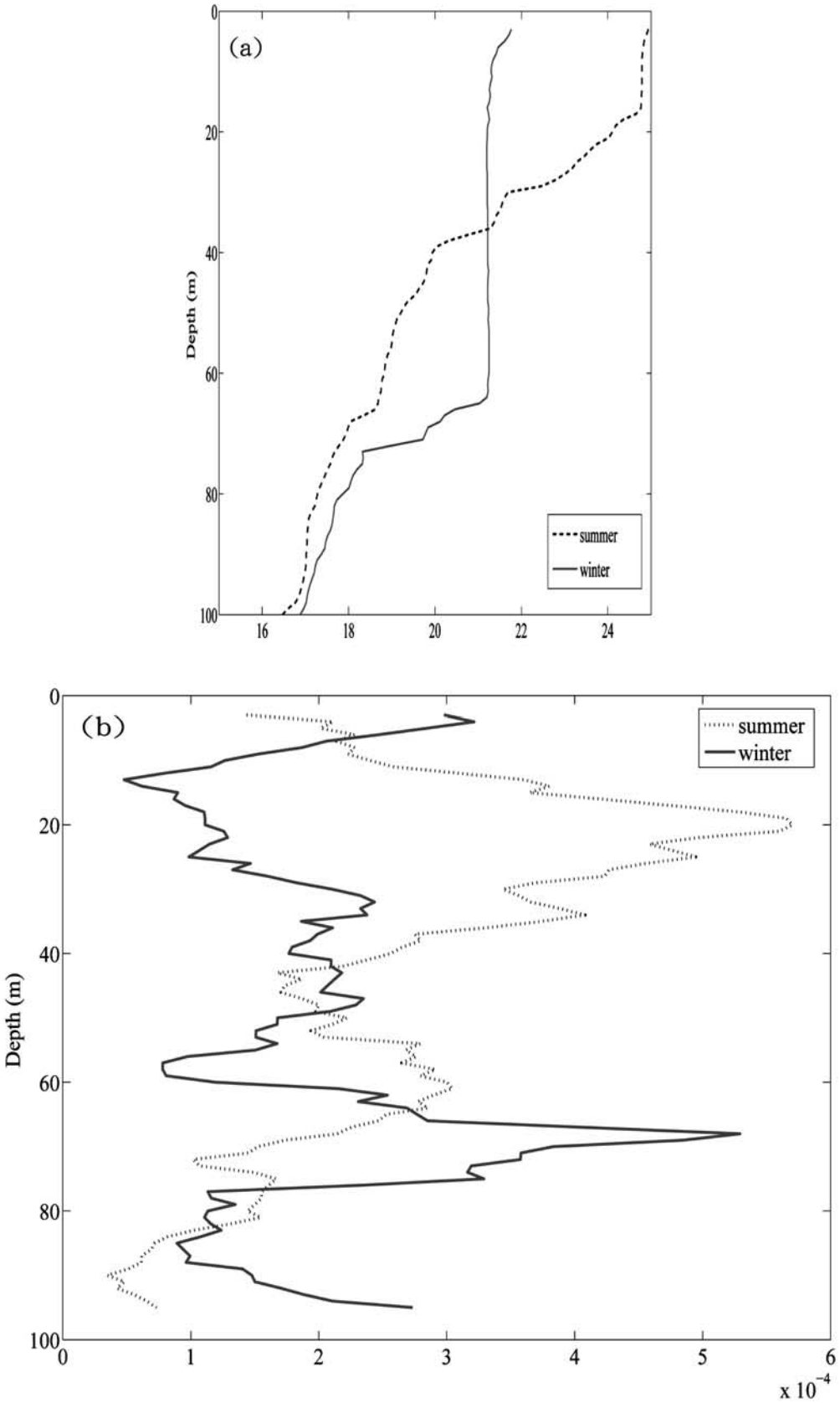

Figure 7. (a) CTD temperature profile in the upper 100 m in summer (dashed line; 122.25°E, 25.33°N) and in winter (solid line; 122.25°E, 25.42°N). (b) Buoyancy frequency squared at the upper 100 m in summer (dashed line) and in winter (solid line).

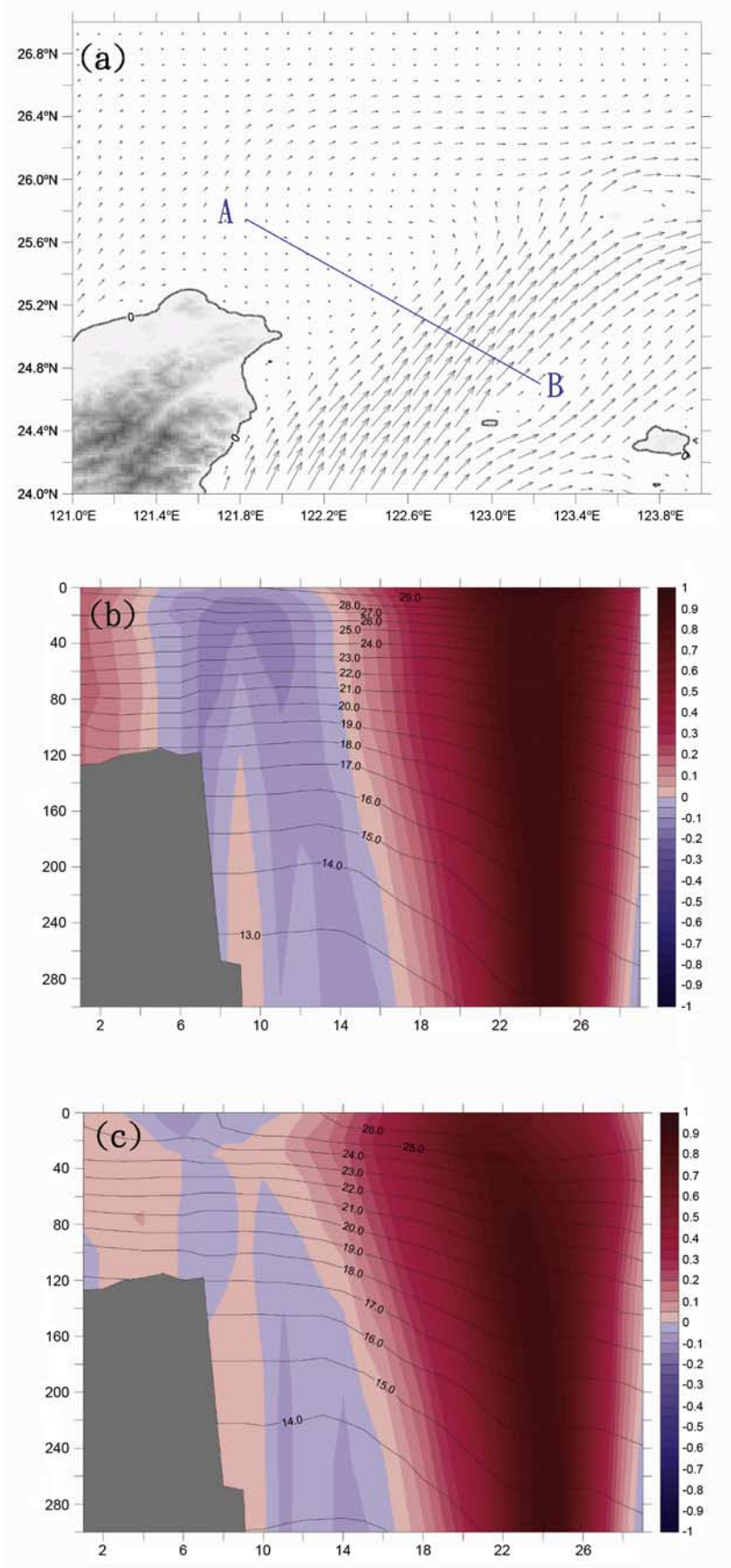

Figure 8. (a) The blue segment AB across the Kuroshio indicates the position of the transection. Vertical section of along-stream velocity together with temperature contours in (b) summer and (c) winter.

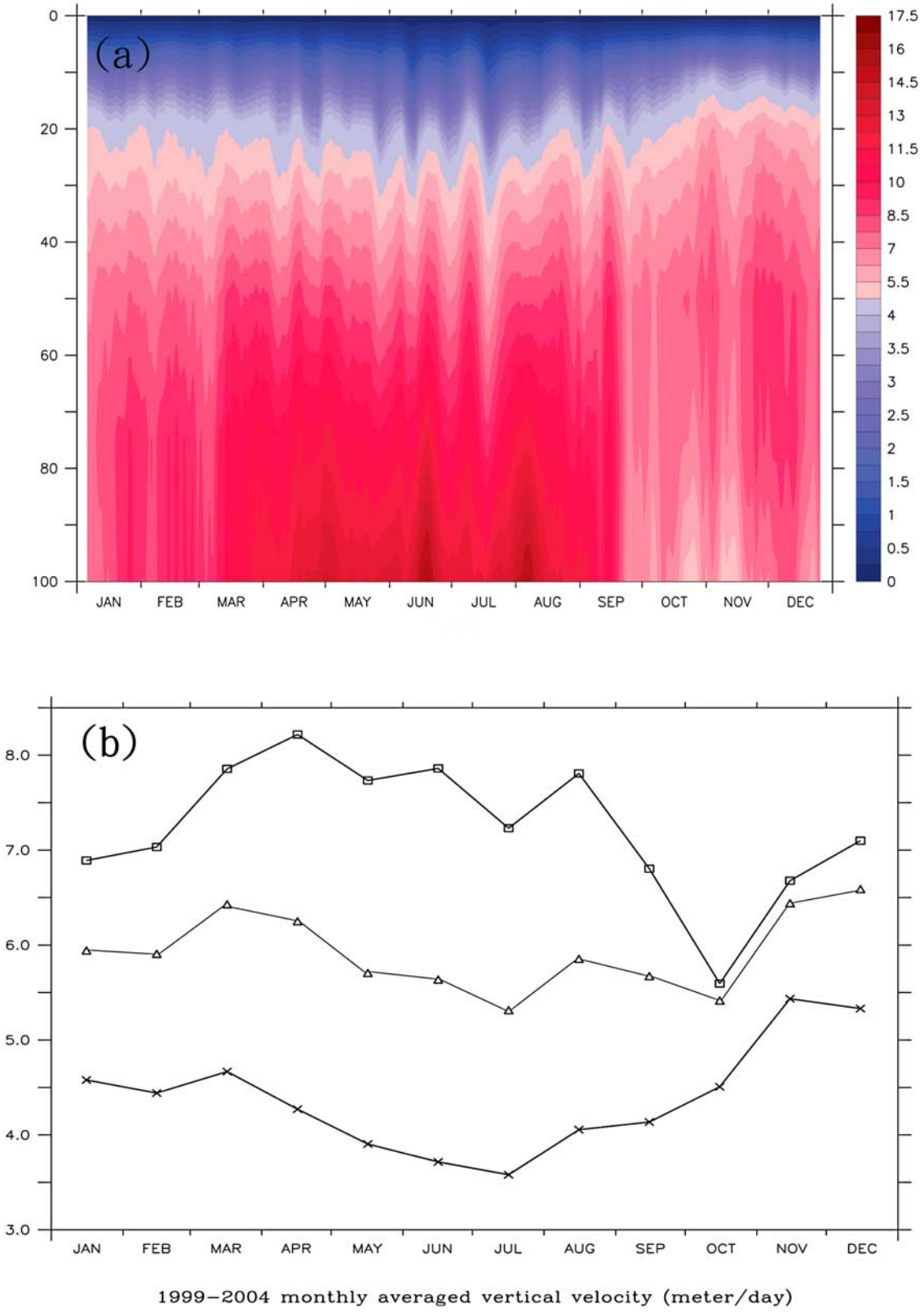

Figure 9. (a) Seasonal variation of the vertical velocity in the upper 100 m based on the model's 10-day running averaged values from 1999 to 2004. (b) Monthly averaged vertical velocity in the upper 100 m (open square), in the top 30 m (cross), and in the upper 60 m (open triangle).

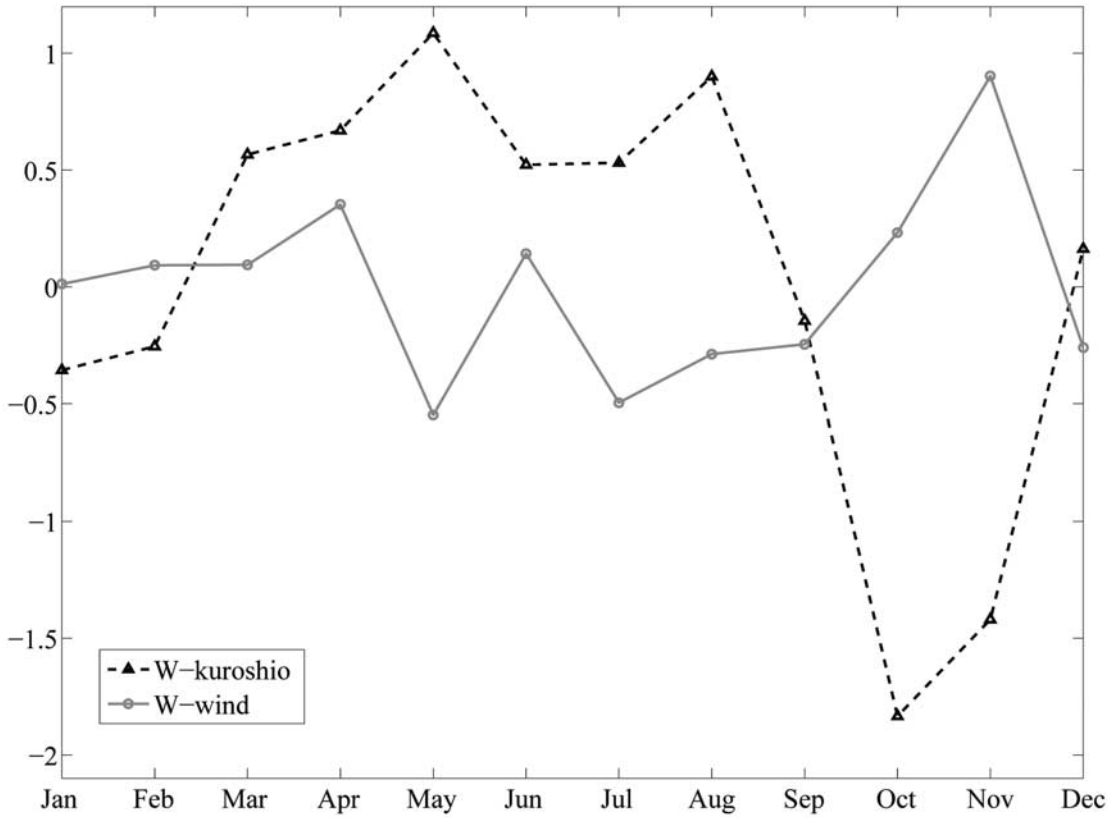

Figure 10. Monthly averaged anomaly w_{kuroshio} (dashed line, mean = 7.5 m/d) and w_{wind} (solid line, mean = −0.3 m/d) from 1999 to 2004 in the upper 100 m.

2004. While upwelling due to the Kuroshio ($w_{\text{kuroshio}} > 0$) prevails throughout the year, the w_{kuroshio} shows positive (negative) anomalies in summer (winter). Figure 10 shows that this seasonal variability is accounted for by the contribution (approximately 40% for the upwelling averaged from surface to a depth of 100 m) from the w_{wind}, which generally forces downwelling in summer and upwelling in winter.

4. Conclusion

[17] This paper uses a high-resolution numerical model and simple Ekman models to explain the seasonal variability of upwelling over the outer shelf and shelf break off the northeastern coast of Taiwan. The circulation in this region is complicated by the active interaction of the Kuroshio with the shelf waters. There is a similar seasonal tendency in the top 30 m in the nutrient data (Figure 2) and in the model (Figure 9). The model shows maximum upwelling during winter and minimum during summer. The nutrient data show higher values in winter and early spring, which are most likely produced by upwelling, and low values in summer indicative of weak or even negative vertical velocity. Wind forcing is responsible for this near-surface seasonal tendency. That is, the wind-induced vertical velocity w_{wind} dominates the vertical velocity on the shelf where it is positive in winter and negative in summer (Figure 3). On the other hand, in addition to w_{wind}, vertical velocity induced by the Kuroshio (w_{kuroshio}) also plays an important role in the upwelling region farther offshore. The w_{kuroshio} shows a year-round upwelling which is stronger in summer than in winter, and a fairly substantial portion (about 40%) of this seasonal variability is due to w_{wind}. The w_{wind} produces upwelling in winter but downwelling in summer. The result is a bimodal behavior of the seasonal upwelling with opposite seasonal tendencies of upwelling at different depths (Figure 9). The bimodal behavior is caused by the upper 30 m being influenced by the local wind stress curl that is generally weaker and negative in summer but becomes stronger and positive during winter. It will be interesting to explain what causes the remaining seasonal variability (approximately 60%) in w_{kuroshio}; this is left for future research [e.g., *Wu et al.*, 2008].

[18] The model provides the upwelling transports in the area which can be useful to the regional oceanographic community for further research. Over the upwelling region, the model results show that the average vertical velocity in the top 30 m is 2.9 m/d in summer and 4 m/d in winter, while the annual mean is 3.4 m/d. The average vertical velocity in the upper 100 m is 7.4 m/d in summer, 6.1 m/d in winter, and 6.9 m/d yearly.

[19] **Acknowledgments.** The authors would like to thank the two anonymous reviewers for their careful review of the manuscript and detailed suggestions to improve the manuscript. Gracious thanks are extended to K.-K. Liu at National Central University and H.-F. Lu for useful discussions. Author C. R. W. was supported by the National Science Council, Taiwan, under grants NSC 95-2611-M-003-001-MY3 and NSC 97-2628-M-008-001.

References

Chao, S.-Y. (1991), Circulation of the East China Sea, a numerical study, *J. Oceanogr.*, *42*, 23–295.

Chen, C. T. A. (1996), The Kuroshio intermediate water is the major source of nutrients on the East China Sea continental shelf, *Oceanol. Acta*, *5*, 523–527.

Fan, K. L. (1980), On the upwelling off northeastern shore of Taiwan, *Acta Oceanogr. Taiwan.*, *11*, 105–117.

Gill, A. E. (1982), *Atmosphere-Ocean Dynamics*, pp. 320–321, Academic, San Diego, Calif.

Gong, G. C., C. Z. Shyu, W. H. Shiu, and K. K. Liu (1992), Temperature fluctuation of the cold eddy off the northeastern Taiwan: June–December, 1990, *Acta Oceanogr. Taiwan.*, *28*, 118–127.

Gong, G. C., et al. (1997), Effect of Kuroshio intrusion on the chlorophyll distribution in the southern East China Sea north of Taiwan during Spring, 1993, *Cont. Shelf Res.*, *17*, 79–94, doi:10.1016/0278-4343(96)00022-2.

Hsu, D. Y. (2005), The temporal-spatial variation of bacterioplankton in the upwelling region, East China Sea, M. S. dissertation, 50 pp., Natl. Taiwan Univ, Taipei.

Kagimoto, T., and T. Yamagata (1997), Seasonal transport variations of the Kuroshio: An OGCM simulation, *J. Phys. Oceanogr.*, *27*, 403–418, doi:10.1175/1520-0485(1997)027<0403:STVOTK>2.0.CO;2.

Liu, K. K., et al. (1992), The year-round upwelling at the shelf break near the northern tip of Taiwan as evidenced by chemical hydrography, *Terr. Atmos. Oceanic Sci.*, *3*, 243–276.

Mellor, G. L. (2004), *Users Guide for a Three-Dimensional, Primitive Equation, Numerical Ocean Model*, 56 pp., Program in Atmos. and Oceanic Sci., Princeton Univ., Princeton, N. J.

Tang, T. Y., J. H. Tai, and Y. J. Yang (2000), The flow pattern north of Taiwan and the migration of the Kuroshio, *Cont. Shelf Res.*, *20*, 349–371, doi:10.1016/S0278-4343(99)00076-X.

Wu, C.-R., and Y. C. Hsin (2005), Volume transport through the Taiwan Strait: A numerical study, *Terr. Atmos. Oceanic Sci.*, *16*, 377–391.

Wu, C.-R., H.-F. Lu, and S.-Y. Chao (2008), A numerical study on the formation of upwelling off northeast Taiwan, *J. Geophys. Res.*, *113*, C08025, doi:10.1029/2007JC004697.

Y.-L. Chang and C.-R. Wu, Department of Earth Sciences, National Taiwan Normal University, 88, Section 4 Ting-Chou Road, Taipei 11677, Taiwan. (cwu@ntnu.edu.tw)

L.-Y. Oey, Program in Atmospheric and Oceanic Sciences, Princeton University, 14 Taunton Court, Princeton, NJ 08550, USA.